Available online at www.sciencedirect.com
ScienceDirect
Catalysis Today 118 (2006) 433–439
CATALYSIS TODAY
www.elsevier.com/locate/cattod

Comparative photocatalytic behavior of Ta catalysts prepared by d.c.-sputtering, sol–gel and grafting in acetone degradation

Vasile I. Parvulescu [a,*], Claudia Visinescu [a,b], Viorica Parvulescu [a], Victor Marcu [c], Francis Levy [b,*]

[a] University of Bucharest, Faculty of Chemistry, Department of Chemical Technology and Catalysis, Bdul Regina Elisabeta 4-12, Bucharest 70346, Romania
[b] Ecole Polytechnique de Lausanne, Department of Physics, 1015 Lausanne, Swiss
[c] Israel Electric Corporation, Orot Rabin Power Station, P.O. Box 2062, Hadera, Israel

Available online 28 August 2006

Abstract

Ta-doped photocatalysts were prepared using three different techniques: reactive d.c.-magnetron sputtering, sol–gel and grafting of tantalum on MCM-41 and TiO_2. The composition of the catalysts prepared by reactive d.c.-magnetron sputtering consisted in tantalum and titania, while that of sol–gel and grafted catalysts of Ta–titania–silica mixed oxides. The characterization of these catalysts was carried out using the adsorption-desorption isotherms of N_2 at 77 K, X-ray diffraction (XRD) patterns, small-angle X-ray scattering (SAXS), atomic force microscopy (AFM), XPS, TEM, and ^{29}Si- and ^{181}Ta-CP/MAS NMR spectra. The behavior of these photocatalysts was checked in acetone degradation. The photocatalytic tests indicate that, depending on the preparation conditions and tantalum content, an enhancement of the activity occurs as compared with pure titania. Sol–gel and Ta-grafted MCM and TiO_2 catalysts exhibited a rather poor activity, which was correlated with the lack of crystallinity of titania.

Keywords: Ta-doped photocatalysts; Reactive d.c.-magnetron sputtering; Sol–gel and grafting; XRD; AFM; XPS; Acetone photodegradation

1. Introduction

Titanium dioxide is largely used as photocatalyst. Several characteristics concur to this fact: high photocatalytic efficiency, physical and chemical stability, low cost and low toxicity. In addition to its wide bandgap, titania exhibits many other interesting properties, such as transparency to visible light, a high refractive index and a low absorption coefficient. All these properties make TiO_2 a good candidate for potential applications in air clean-up and water purification [1,2].

Doping of titania photocatalysts with a proper ion is expected to result in a continuous improvement of the photocatalytic activity, by increasing the lifetime of the electron/hole pairs. Literature already reported several attempts in this sense [3–7]. However, the role of dopants in increasing photocatalytic activity is very complex and not completely understood, requesting further investigations.

According to the electronic theory of semiconductors, doping titania with ions of higher than four valence leads to an upward shift of the Fermi level. As a direct consequence, the surface barrier becomes higher and the space charge region narrower and the electron–hole pairs photogenerated within this region are more efficiently separated [8]. Based on its intrinsic characteristics tantalum can be a very good candidate to promote such behavior.

The aim of this paper is to compare the catalytic behavior of tantalum doped-catalysts prepared using several procedures: reactive d.c.-magnetron sputtering technique (a typical procedure to prepare thin films [9,10]), sol–gel and grafting of tantalum on a mesoporous catalyst containing titania. The possibility to produce photocatalysts by deposition of titania thin films on low-cost materials, such as glasses, makes it even more attractive for various applications [11–13], while sol–gel is largely used for preparing dispersed oxide catalysts.

These photocatalysts were tested in the photocatalytic decomposition of acetone, a volatile organic compound that creates serious problems in insufficiently aerated indoor environments. The adsorption and the photocatalytic degradation

* Corresponding authors.
E-mail address: v_parvulescu@yahoo.com (V.I. Parvulescu).

0920-5861/$ – see front matter © 2006 Elsevier B.V. All rights reserved.
doi:10.1016/j.cattod.2006.07.035

of acetone on pure TiO_2 have been previously studied. The titania catalysts used in these studies were those available on the market (as Degussa P25), those prepared by titanium precursors precipitation [14,15] or by d.c.-sputtering [10].

2. Experimental

Titania-based thin films were prepared by reactive d.c.-magnetron sputtering, using a Sputtron II (Balzers) equipment. The distance between the substrate holder and the titanium target, inside the deposition chamber, was 7 cm. The titanium (99.7% titanium, from Lesker) disk-shaped target was of 10 cm diameter and allowed the modification with 1 up to 6 Ta inserts (99.9% purity). The size of one tantalum insert corresponded to 0.25% of the total area of the target. The titanium target was connected to a negative d.c. bias source, such that it was bombarded by positively charged ions present in the plasma. The plasma discharge was generated under a current intensity of 0.2 A, and a potential of 450 V. Before each preparation, the deposition chamber was evacuated to a pressure of 5×10^{-6} mbar and the target surface was cleaned using plasma generated in a pure argon atmosphere. The reactive gas consisted of oxygen (Carbagas, purity 48, without oils and fats), while argon was used as inert gas (Carbagas, purity 48, oil and fats free). The total operating pressure was fixed at 5×10^{-3} mbar and the reactive gas pressure at 50% of the total operating pressure. Microscope glass slides (RE-WA Lehmann-Schmidt) were used as substrates. The glass slides were degreased by rinsing with isopropylic alcohol in an ultrasonic bath and then dried using a N_2 gun. The temperature of the substrates during the depositions was maintained at 573 ± 10 K, or at 500 ± 10 K for the sample Ta-1.61. The denomination of the samples includes the name of the dopant and its atomic percentage in the film composition (x), as Ta-x (Table 1).

The sol–gel technique was used to prepare Ta_2O_5 (2 wt.%)–TiO_2–SiO_2 catalysts. TEOS, Ti isopropoxide, and tantalum (V) ethoxide were used as precursors. All the solvents and chemicals used for the photocatalysts preparation were reagents grade from Fluka. The silica–titania sol was obtained using the following composition TEOS:TiIP:H_2O:C_2H_5OH = 1:0.3:4.5:50. Tantalum ethoxide was added to the formed sol–gel resulting in a transparent gel. At that moment the surfactant was also added. The concentration of tantalum has been calculated to correspond to the highest loading in the d.c.-sputtered catalysts (Table 1). Gelification was carried out at room temperature, and the resulting gel was dried under vacuum at 80 °C, and calcined at 600 °C for 5 h. Two families of quaternary ammonium salts, $C_{16}H_{33}(CH_3)_3NBr$ and $(C_{16}H_{33})_4NBr$ were used as surfactants. Accordingly, the catalysts were denoted as Ta-16 or Ta-4-16.

In addition to these, two more catalysts: Ta-MCM-41 and Ta–TiO_2 were prepared by grafting tantalum from an alcoholic solution of tantalum ethoxide to the respective supports. MCM-41 was prepared according to a well known procedure [16]. TiO_2 was prepared by sol–gel from a solution of TiIP using the following composition: TiIP:H_2O:C_3H_7OH = 1:4:30. Gelification was carried out at room temperature, and the resulting gel was dried under vacuum at 80 °C, and calcined at 400 °C for 5 h. Like for the sol–gel catalysts, the content in tantalum was calculated to correspond to the highest loading in d.c.-sputtered catalysts (Table 1).

The characterization of these catalysts was carried out using the adsorption–desorption isotherms of N_2 at 77 K, X-ray diffraction (XRD) patterns, small-angle X-ray scattering (SAXS), atomic force microscopy (AFM), XPS, TEM, and ^{29}Si- and ^{181}Ta-CP/MAS NMR spectra. Surface area measurements and pore size distributions were obtained from adsorption–desorption isotherms of N_2 at −196 °C using a Micromeritics ASAP 2000 apparatus following evacuation of the samples at 423 K for 12 h. The film thickness was measured with an Alphastep 500 Surface profiler (Tencor Instruments) coupled to a computer. XRD patterns were obtained using a Rigaku diffractometer, the Cu Kα radiation (λ = 1.5418 Å) being provided by a Philips X-ray source. The measurements were made in grazing incidence geometry, at an angle of 5° between the X-ray direction and the film surface. SAXS experiments were performed with an evacuated Kratky compact camera mounted on a Siemens rotating copper anode (6 kW) with a take-off angle of 3°. Selection of Cu Kα radiation was achieved using a Ni filter and completed by electronic discrimination. Precise values of channel width and sample-to-detector distances were obtained by measuring calibration standards, namely rat-tail collagen and crystalline monodisperse oligomers having as repeating unit (–F–O–F–O–F–CO–), where F represents a para-linked aromatic moeity. The powders were measured in Mark glass capillaries 1 mm in diameter and acquisition times of 1800 s were used throughout. The XPS spectra were recorded using a SSI X probe FISONS spectrometer (SSX −100/206) with monochromated Al Kα radiation. The spectrometer energy scale was calibrated using the $Au4f_{7/2}$

Table 1
The tantalum content of the investigated catasysts, as given by EPMA

Catalyst	Number of tantalum insertions	Ta (at.%)	Catalyst	Ta (at.%)	Surface area ($m^2\ g^{-1}$)
Ta-0	–	–	Ta-16	1.63	982
Ta-0.28	1	0.28	Ta-4-16	1.63	768
Ta-0.46	2	0.46	Ta-MCM	1.58	945
Ta-0.60	3	0.60	Ta-TiO_2	1.56	8
Ta-1.31	4	1.31			
Ta-1.26	5	1.26			
Ta-1.42	6	1.42			
Ta-1.61	3	1.61			

peak (binding energy 84.0 eV). For the calculation of the binding energies, the C 1s at 284.8 eV was used as an internal standard. The peaks assigned to Ta 4d, Ta 4f, Ti 2p, Si 2p and O 1s levels were analyzed. The ^{29}Si Magic angle spinning (MAS) NMR experiments were performed at room temperature on a Bruker ASX100 spectrometer (2.33 T) operating at a Larmor frequency of 19.89 MHz for ^{29}Si with a 4 mm probehead. The ^{29}Si MAS NMR spectra were obtained at 5 kHz spinning rate using a single pulse excitation ($\pi/10$) with a recycle delay of 15 s to prevent saturation. The ^{29}Si chemical shifts were referenced relative to $Si(CH_3)_4$. The simulations were performed using the DMfit program [17]. AFM measurements were made with a Topometrix Explorer AFM in the non-contact mode. UV–vis spectra were collected using a Cary 500 Scan (Varian) spectrometer. For the determination of the *Eg* values, the wavenumbers at which light absorption became zero was taken into account. The composition of the films was determined by electron probe microanalysis (EPMA). TEM were obtained using a JEOL 200 CX transmission electron microscope operated at 120 kV. Samples were embedded in a polymeric resin and cut into sections as approximately 20 nm thick with an ultramicrotome. They were then deposited on holey carbon copper grid before TEM observation.

Photocatalytic tests were performed in a flow system, using a water-cooled quartz reactor. The catalysts were irradiated using a Philips HPK 125 W UV-lamp. Catalyst platelets of 1.60–2.30 cm^2 surface area were placed inside the reactor, perpendicular to the light propagation direction, the titania-based film being exposed to the UV radiation. Purified and dried air, containing 34% acetone was sent to the reactor at a flow rate of 13.3 cm^3 min^{-1}. The gas flow circulation rate was maintained constant during the experiments using a pump. The reactor was coupled on line to a Fisher-Rosemount gas analyzer, equipped with a CO_2 detector. The gas analyzer was calibrated before each test. Before the UV irradiation, an acetone containing air stream was purged through the reactor over the catalysts for 20 min. No catalytic reaction products were detected in the absence of the UV radiation. The starting time of each catalytic experiment was considered the moment when the UV lamp was turned on. The activity was expressed as steady-state conversion % per surface area of the platelets. The conversion was calculated as the number of moles of acetone transformed in CO_2 relative to the number of moles of acetone present in the gas mixture. The exposure time was at least 200 min. The residue was analysed with a Hewlett-Packard gas chromatograph, model 5890 series II, coupled with a mass spectrometer AMD-402.

3. Results

Table 1 compiles the composition and surface areas of the investigated photocatalysts. Although the tantalum loading was close for catalysts prepared by various methods, i.e. Ta-1.42 and Ta-1.61 prepared by d.c.-sputtering, Ta-16 and Ta-4-16 prepared by sol–gel, and Ta-MCM and Ta–TiO_2 obtained by grafting, the surface areas of these samples were very different.

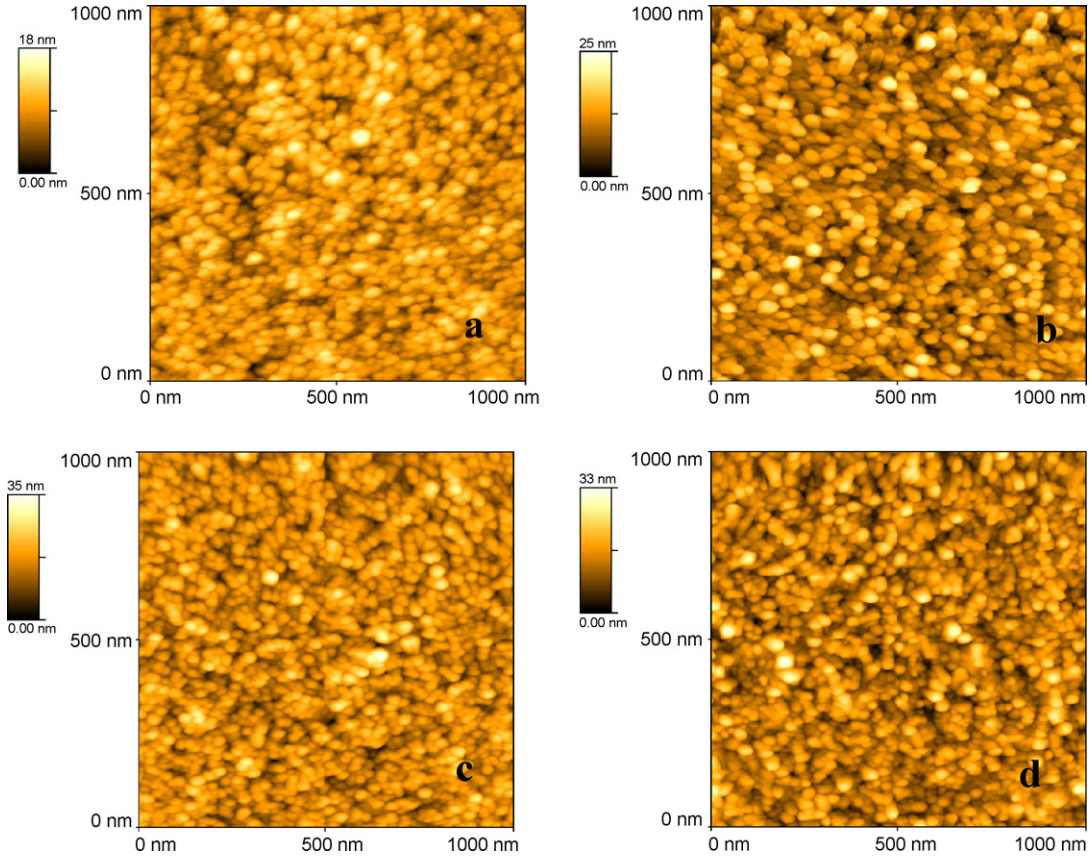

Fig. 1. AFM images of samples: (a) Ta-0.60; (b) Ta-1.61; (c) Ta-1.26; (d) Ta-1.42 on a scale 25,000 nm^2.

The surface area of d.c.-sputtered catalysts was always lower than 2.8 $m^2\ g^{-1}$, a small surface area was also measured for Ta–TiO_2, while those of the other catalysts exceeded 750 $m^2\ g^{-1}$. Ta-16 and Ta-MCM exhibited a mesoporous texture with a monomodal pore size distribution (3.4 and 2.8 nm, respectively), while Ta-4-16 a bimodal pore size distribution (pores with 2.8 and 22 nm). The texture of Ta-16 and Ta-MCM was confirmed by SAXS experiments.

For the d.c.-sputtered catalysts, the thickness of the deposited films, as measured with the Alphastep profiler, varied between 150 and 300 nm. AFM analysis of these samples indicated a polycrystalline structure consisting of superposed round-shape grains (Fig. 1). The morphology of the surface does not seem to depend either on the deposition conditions or on the tantalum content. The preparation conditions induced only very small differences in wrapping of the grains. However, among the investigated samples, Ta-0.60 and Ta-1.61 showed the smoothest surface, the differences between the lowest and the highest points of the surface being of only 11.91 and 10.54 nm, respectively.

XRD patterns presented in Fig. 2a indicate that all the d.c.-sputtered samples are crystalline. XRD peaks are due to the crystalline TiO_2 (anatase). However, the rather low intensity of the lines (see Ta-0), may account for the existence of amorphous titania, too. The addition of tantalum, and the increase of its content, improved the crystallinity of these catalysts. Furthermore, the increase of the tantalum content led to a phase transition, small amounts of rutile being identified as well. Sol–gel prepared catalysts, i.e. Ta-16, Ta-4–16, Ta–TiO_2 (Fig. 2b) were essentially amorphous. Except for the large peak in the range 20°–30° 2 theta assigned to silica, no other reflexion line has been identified. A similar picture was obtained for Ta-MCM: except for the line assigned to MCM structure, no other lines have been detected (pattern not shown). As expected, in none of these XRD patterns tantalum has been identified. TEM analysis was in line with these measurements.

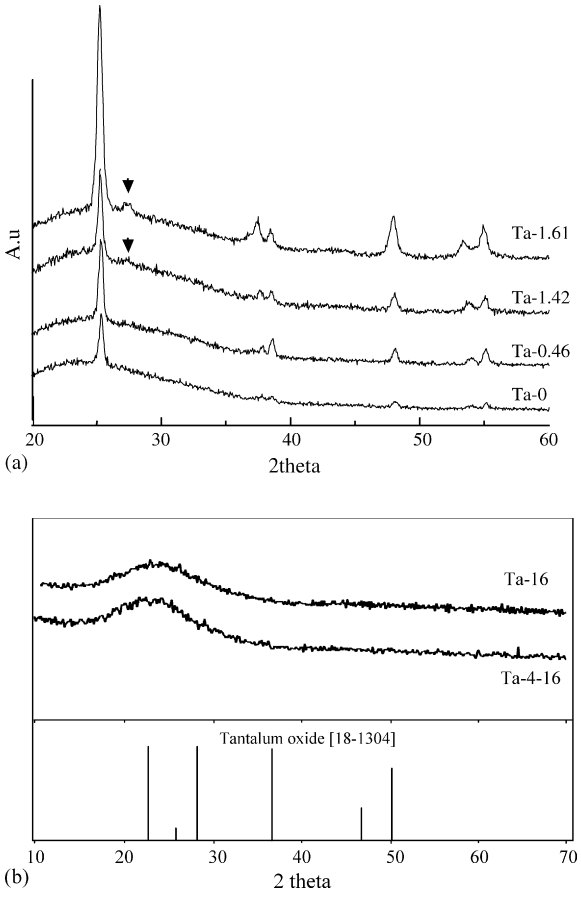

Fig. 2. a. XRD patterns of d.c.-sputtered catalysts (↓ = rutile) b. XRD patterns of Ta-16 and Ta-4-16 catalysts.

On the opposite, the presence of tantalum has been detected in XPS measurements. As expected, the binding energies corresponding to Ta $4f_{7/2}$ level exhibit typical values for Ta^{5+} [18]. XPS binding energies and comparative chemical and XPS determined atomic ratios are given in Table 2. For the d.c.-sputtered catalysts, XPS atomic Ta/Ti ratios approximate very well the values determined from chemical analysis. A good agreement resulted for Ta-16 and Ta-4-16 catalysts as well. For Ta-MCM, the higher Ta/Ti ratio could be due to the fact that the tantalum is spread more evenly over the surface and the titanium is less exposed, when compared with multilayers of Ta_2O_5 in small clusters. The values measured for Ta–TiO_2 account for a certain agglomeration of Ta on titania surface, although no XRD reflexion line has been detected in the recorded patterns. The lack of the bulk TiO_2 phase is also responsible for this value. However, these results are only qualitative.

XPS analysis of these samples in the region of Ti2p doublet featured symmetric curves. The binding energies determined for these levels were very close to those reported in literature for titanium dioxide [19,20]. A different picture is shown by both Ta-16 and Ta-4-16, and Ta-MCM catalysts, in which the higher values may account for a better incorporation of titanium in the solid network [21].

^{181}Ta NMR spectra gave no information about the state of tantalum because of the high level of noise. On the contrary, the ^{29}Si NMR spectra of Ta-16, Ta-4-16 and Ta-MCM contained well defined signals with a major peak centred around −109 ppm. Spectra corresponded to Ta-16 and Ta-4-16 catalysts were fitted on the basis of three contributions (i.e.

Table 2
XPS binding energies and XPS determined Ta/Ti atomic ratios

Catalyst	XPS binding energy (eV)			Ta/Ti atomic ratio × 10^3	
	Ta $4f_{7/2}$	Si $2p_{3/2}$	Ti(2p3/2)	Chemical analysis	XPS
Ta-0	–	–	458.6	–	–
Ta-0.28	26.4	–	458.6	8.46	8.32
Ta-0.46	26.4	–	458.6	12.70	15.49
Ta-0.60	26.4	–	458.6	18.38	19.64
Ta-1.31	26.4	–	458.6	41.18	41.39
Ta-1.26	26.4	–	458.6	39.56	41.37
Ta-1.42	26.4	–	458.6	44.82	51.55
Ta-1.61	26.4	–	458.6	51.17	61.89
Ta-16	26.4	103.2	459.0	106.70	126.12
Ta-4-16	26.4	103.2	459.0	106.13	137.93
Ta-MCM	26.5	103.4	459.2	118.44	176.42
Ta-TiO_2	26.5	–	458.6	51.12	140.35

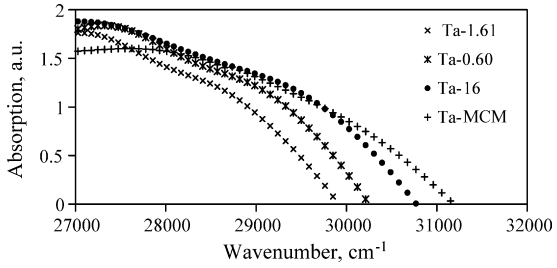

Fig. 3. UV–vis spectra of the investigated catalysts.

Q_4, Q_3, and Q_2 species) while that of Ta-MCM on the basis of two contributions (i.e. Q_4 and Q_3 species). These spectra indicated that the polymerization of silicon decreased in the order Ta-MCM > Ta-16 > Ta-4-16. Since the composition of these catalysts is rather close, an explanation should consider the contribution of the surfactant and the presence of tantalum for Ta-16 and Ta-4-16.

Typical UV–vis spectra of the investigated samples are given in Fig. 3. UV–vis spectra of the thin films prepared by sputtering exhibit a shoulder in the range 28,250–28,550 cm^{-1}, which, according to the literature data, can be assigned to nanosized anatase particles [22]. Light absorption corresponding to the bandgap of the semiconductors is observed at wavelengths in the range 29,850–31,350 cm^{-1} (see Fig. 3), values slightly higher than that corresponding to powder anatase, 28,514 cm^{-1} [23]. It is interesting to note that even the sample containing undoped anatase presented an *Eg* of 3.9 eV, larger than the bandgap energies of both rutile and anatase in powder form. This is also the highest bandgap energy in this catalysts series. Doping with Ta ions resulted in a slight decrease of the semiconductor *Eg*, which, for the doped samples, ranged between 3.71 eV for Ta-1.61 and 3.80 eV for Ta-0.28 and 3.87 eV for Ta-1.26. Exception made sol–gel prepared catalysts and Ta-MCM for which the *Eg* exceeded 3.9 eV. The large blue shift observed for these catalysts is due to the quantum-size effect, produced by the small dimensions of the titania crystallites. The results of the UV–vis spectroscopy are confirmed by XRD patterns: the broadened peaks present there are a proof of the low crystallinity of titania films.

Fig. 4 shows the photocatalytic behavior of the investigated catalysts in the decomposition of acetone, as a function of the tantalum catalyst. The catalysts reached the steady state after approximately 100 min from the beginning of the reaction. The conversion increased rather fast during the first 50 min, then slowly reached a constant value. Mass spectrometric analysis of gases and the residual liquid in the photoreactor indicated that, for d.c.-sputtered catalysts, under the investigated conditions, CO_2 was the only product. No CO or intermediate decomposition products of acetone have been detected on these catalysts. On the opposite, on Ta-16, Ta-4-16 and Ta-MCM photocatalysts the analysis of the residual liquid indicated, in addition to acetone, the formation of acetic acid (5% versus total conversion of acetone) after 200 min.

Data presented in Fig. 4a show that the samples doped under the same conditions exhibit a maximum of the conversion on tantalum content with a maximum corresponding to 0.60 at.%

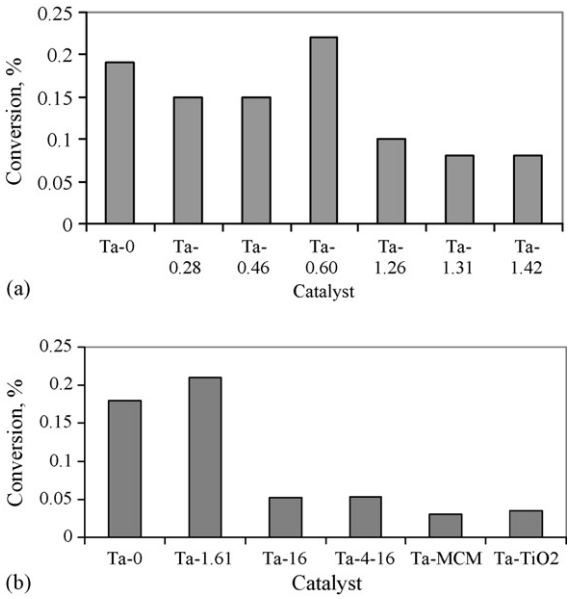

Fig. 4. Catalytic activity of the investigated photocatalysts, after reaching the steady state: (a) d.c.-sputtered catalysts; (b) Ta-16, Ta-4-16 and Ta-MCM as compared with Ta-0 and Ta-1.61.

Ta (sample Ta-0.60). Lower and even higher Ta loadings led to a photocatalytic activity inferior to that of the undoped sample. The decrease of the conversion for further increases in the Ta amount may be associated with the formation of Ta aggregates. The value of the conversion determined for Ta-1.61 evidences the effect of the preparation condition, this sample being obtained at a lower substrate temperature.

Catalysts prepared by sol–gel or grafting i.e. Ta-16, Ta-4-16, Ta–TiO_2 and Ta-MCM exhibited lower photocatalytic activity compared with the d.c.-sputtered ones.

The reproducibility of these results has been checked running fresh catalysts with the same characteristics five times in the same photocatalytic conditions. The differences found under these conditions were smaller than 3%.

Fig. 5 presents a plot of the conversion versus bandgap energy of the catalysts. The best photocatalytic activity corresponded to the samples with the lowest *Eg* values. It follows that an increase of the bandgap energy leads to a decrease of the photocatalytic activity. That means that the

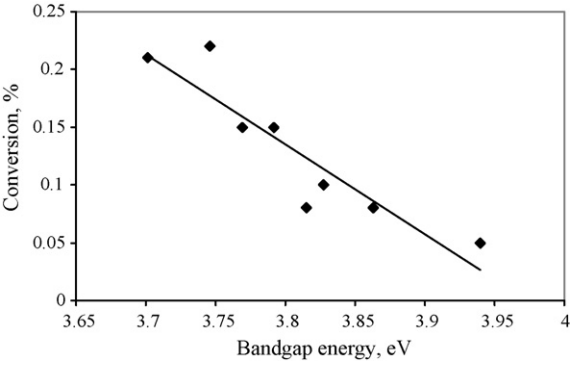

Fig. 5. Correlation between the photocatalytic activity and bandgap energy of the photocatalysts.

catalytic performance is proportional to the catalyst capacity to use UV–vis radiation of lower energy.

4. Discussions

Photocatalysts prepared using the d.c. reactive sputtering deposition method corresponded to thin titania films made of nanosized crystallites, as demonstrated by the blue shift of the bandgap absorption and the broadening of the diffraction peaks. These films were made mainly of anatase, and doping with Ta for relatively high loadings (higher than 1.42 at.% Ta) led to the appearance of rutile peaks in the diffraction patterns. The presence of tantalum enhanced the crystallinity of these samples, as well. Photocatalysts prepared by sol–gel or Ta anchoring on MCM-41 or on a low surface TiO_2 corresponded to amorphous materials in which no diffraction line of anatase or rutile have been detected.

The presence of Ta-ions influenced the surface morphology only in the case of the thin films. The highest conversions are exhibited by the samples with the smoothest surface, as given by AFM. Indeed, for samples Ta-0.60 and Ta-1.61, the differences between the lowest and the highest points of the surface were 11.91 and 10.54 nm, respectively, while for the rest of the samples the surface roughness was more than 50% higher. Powder catalysts exhibited very poor photocatalytic behavior irrespective of the way they have been prepared.

The photocatalytic activity of the catalysts depends on several factors, among which the preparation conditions and the loading with tantalum were the most important. For a series of catalysts prepared under the same conditions, but with a different Ta content, the conversion followed a dependence with a maximum. From the data reported in the literature [6,7], it appears that a volcano-type curve is a rather typical behavior for the titania catalysts doped with ions of valence higher than 4.

The photocatalytic results also confirmed the importance of the anatase in the degradation of acetone. However, in addition to anatase, small amounts of rutile (see sample Ta-1.61) seem to have a beneficial influence on the activity. Ohno et al. [24] also observed a synergetic effect in the photocatalytic decomposition of naphtalene when anatase and rutile particles were in contact. Although the promotion by co-existing anatase-rutile reported by Ohno et al. [24] does not appear applicable to this system, the results are in the same line.

As mentioned, XRD patterns of powdered catalysts contained no diffraction line assigned to anatase and their poor photocatalytic behavior may be associated with this fact. The presence of tantalum had no positive effect, although the Ta/Ti ratio was comparable with that in d.c.-sputtered films. However, it is worth noting that in these catalysts titania was well dispersed and no structural characterization gave any indication to the fact that tantalum interacted indeed with titania in these cases.

In addition, Ta-16, Ta-4-16 and Ta-MCM catalysts exhibit a very high surface area and a pore blocking by capillary condensation of the water vapors resulting from the reaction may suppress the photoactivity in the acetone degradation.

On the other side, the photoactivity of these catalysts was found to be directly proportional to the width of the bandgap of these semiconductors. However, no correlation between the Ta loading and the magnitude of the bandgap could be established. Although the activity of the most active doped samples (Ta-0.60 and Ta-1.61) is only slightly higher than that of the undoped sample, the doped samples exhibit a better ability to use UV light of lower energy.

These data indicate that depending on the way the catalysts have been prepared Ta may exhibit a positive effect. However, the role played by the Ta ions in the modification of titania photocatalytic properties is still unclear, as is that of other ions with higher valence than Ti^{4+}. The electronic theory of semiconductors stipulates that doping titania with ions of valence higher than four leads to an upward shift of the Fermi level. As the dopant concentration increases, the surface barrier becomes higher and the space charge region narrower. The electron–hole pairs photogenerated within this region are efficiently separated by the large electric field across the barrier, before having the chance to recombine [8]. Thus, it would appear that increasing the doping ion amount would result in a continuous improvement of the photocatalytic activity, by increasing the lifetime of the electron/hole pairs. This is not the case experimentally observed. Moreover, Wilke and Breuer [6] demonstrated that doping TiO_2 with 0.5 at.% Mo^{5+} ions, using a synthesis method based on the sol–gel process, reduced the lifetime of the electrone/hole pairs from 89.3 μs (TiO_2) to about 30 μs.

Summarizing, these results suggest that tantalum is not promoting the performances of the photocatalysts via its intrinsic properties. Doping with tantalum after a certain loading affords better anatase crystals and lower photocatalytic performances. This is consistent with the band gap energy values trends. However, till a certain amount Ta may determine the formation of titania domains with a crystalline structure. The maximum in conversion for Ta-0.60 may account for this behavior.

5. Conclusions

The photocatalytic studies carried out in this study using Ta-doped catalysts prepared by d.c.-sputtering, sol–gel and grafting evidenced the role of titanium-dioxide. Crystalline titania was found only in d.c.-sputtered catalysts, and in consequence these exhibited the higher photocatalytic activity. In addition, the combination of anatase with rutile enhanced the photocatalytic performances of these catalysts.

The addition of Ta affects the TiO_2 (anatase) particle size, although the intrinsic mechanism of this influence is still not very clear. However, data presented in this paper demonstrate that the TiO_2 (anatase) particle size is tuned by the addition of tantalum as promoter. Finally, the most important conclusion of this study is that the formation of titania domains with a crystalline structure have the lowest E_g and the highest photocatalytic activity.

References

[1] N. Fujishima, T.N. Rao, D.A. Tryk, J. Photochem. Photobiol. C 1 (2000) 1.
[2] R. Andreozzi, V. Caprio, A. Insola, Catal. Today 53 (1999) 51.

[3] M. Litter, J.A. Navio, J. Photochem. Photobiol. A 98 (1996) 171.
[4] H. Yamashita, Y. Ichihashi, M. Takeuchi, S. Kishiguchi, M. Asupo, J. Synchr. Rad. 6 (1999) 451.
[5] M.I. Litter, Appl. Catal. B 23 (1999) 89.
[6] K. Wilke, H.D. Breuer, J. Photochem. Photobiol. A 121 (1999) 49.
[7] F. Kiriakidou, D.I. Kondarides, X.E. Verykios, Catal. Today 54 (1999) 119.
[8] K.E. Karakitsou, X.E. Verykios, J. Phys. Chem. 97 (1993) 1184.
[9] D. Dumitriu, A.R. Bally, C. Ballif, V.I. Pârvulescu, P.E. Schmid, R. Sanjines, F. Levy, Stud. Surf. Sci. Catal. 118 (1998) 485.
[10] D. Dumitriu, A.R. Bally, C. Ballif, P. Hones, P.E. Schmid, R. Sanjines, F. Levy, V.I. Pârvulescu, Appl. Catal. B 25 (2000) 83.
[11] M.L. Sauer, D.F. Ollis, J. Catal. 158 (1996) 570.
[12] E. Piera, J.C. Calpe, E. Brillas, X. Domenech, J. Peral, Appl. Catal. B 27 (2000) 169.
[13] A.J. Maira, K.L. Yeung, J. Soria, J.M. Coronado, C. Belver, C.Y. Lee, V. Augugliaro, Appl. Catal. B 29 (2001) 327.
[14] Y. Li, G. Lu, S. Li, Appl. Catal. A 214 (2001) 179.
[15] N. Serpone, P. Maruthamuthu, P. Pichat, E. Pelizzetti, H. Hidaka, J. Photochem. Photobiol. A 85 (1995) 247.
[16] S. Coman, M. Florea, F. Cocu, V.I. Parvulescu, P.A. Jacobs, C. Danumah, S. Kaliaguine, Chem. Comm. (1999) 2175.
[17] D. Massiot, F. Fayon, M. Capron, I. King, S. Le Calvé, B. Alonso, J.O. Durand, B. Bujoli, Z. Gan, G. Hoatson, Magn. Reson. Chem. 40 (2002) 70.
[18] S.F. Ho, S. Contarini, J.W. Rabalais, J. Phys. Chem. 91 (1987) 4779.
[19] W.E. Slinkard, P.B. Degroot, J. Catal. 68 (1981) 423.
[20] S.O. Saied, J.L. Sullivan, T. Choudhary, C.G. Pierce, Vacuum 38 (1988) 917.
[21] Z. Luan, E.M. Maes, P.A.W. van der Heide, D. Zhao, R.S. Czernuszewicz, L. Kevan, Chem. Mater. 11 (1999) 3680.
[22] E. Duprey, P. Beaunier, M.-A. Springuel-Huet, F. Bozon-Verduraz, J. Fraissard, J.-M. Manoli, J.-M. Bregeault, J. Catal. 165 (1997) 22.
[23] E. Astorino, J.B. Peri, R.J. Willey, G. Busca, J. Catal. 157 (1995) 482.
[24] T. Ohno, K. Sarukawa, K. Tokieda, M. Matsumura, J. Catal. 203 (2001) 82.